Inhibitory neuromuscular transmission to ileal longitudinal muscle predominates in neonatal guinea pigs

Bhavik A. Patel[1,4,5], **Xiaoling Dai**[2], **Joshua E. Burda**[2], **Hong Zhao**[1,3], **Greg M. Swain**[1,3], **James J. Galligan**[2,3], and **Xiaochun Bian**[2]

[1]Department of Chemistry, Michigan State University, East Lansing, MI 48824 USA

[2]Department of Pharmacology and Toxicology, Michigan State University, East Lansing, MI 48824 USA

[3]Neuroscience Program, Michigan State University, East Lansing, MI 48824 USA

[4]Department of Bioengineering, Imperial College London, London, SW7 2AZ, UK

[5]School of Pharmacy and Biomolecular Sciences, University of Brighton, Brighton, BN2 4GJ, UK

Abstract

Background—Inhibitory neurotransmission to the longitudinal muscle is more prominent in the neonatal than in the adult guinea pig small intestine.

Methods—Inhibitory neuromuscular transmission was investigated using *in vitro* ileal longitudinal muscle myenteric plexus (LMMP) preparations made from neonatal (≤ 48 h postnatal) and adult (~ 4 weeks postnatal) guinea pigs.

Key Results—Amperometric measurements of nicotine induced nitric oxide release (measured as an oxidation current) from myenteric ganglia revealed larger currents in neonatal (379 ± 24 pA) vs. adult (119 ± 39 pA, $P < 0.05$) tissues. Nicotine-induced oxidation currents were blocked by the nitric oxide synthase (NOS) inhibitor, nitro-L-arginine (NLA, 100 µM). Nicotine-induced, NLA-sensitive oxidation currents could be detected in the tertiary plexus of neonatal but not adult tissues. Immunohistochemistry demonstrated stronger NOS immunoreactivity in neonatal compared to adult myenteric ganglia. Western blot studies revealed higher levels of NOS in neonatal compared to adult LMMP. Cell counts revealed that the total number of myenteric neurons in the small intestine was greater in adults than in neonatal guinea pigs, however the ratio of NOS:Calbindin neurons was significantly higher in neonatal compared to adult tissues.

Conclusions—NO signaling to the longitudinal muscle is stronger in neonatal compared to adult guinea pig ileum. NOS-containing neurons are diluted postnatally by cholinergic and other, as yet unidentified neuronal subtypes.

Keywords

Postnatal development; autonomic neurotransmission; enteric nervous system

INTRODUCTION

Recent pharmacological evidence suggests that inhibitory neurotransmission to the longitudinal muscle is relatively more effective in the neonatal compared to the adult guinea

Address for correspondence: Xiaochun Bian Department of Pharmacology and Toxicology Michigan State University East Lansing, MI 24423 Tel: 1-517-355-1711 Fax: 1-517-353-8915 bian@msu.edu.

pig small intestine (1). Delayed excitatory neuromuscular innervation is observed in mouse and rat (2,3). Clinical reports show that constipation is more prevalent in neonates (4,5) and gastrointestinal motility is generally slower in preterm compared to full term babies (6). Knowledge of maturation of neuromuscular transmission in the gastrointestinal (GI) tract is important since pediatric motility disturbances place a large burden on the affected children and their families.

Neuromuscular transmission is controlled by the enteric nervous system (ENS) and the longitudinal and circular muscle layers are supplied by myenteric motorneurons (7). In the adult guinea pig ileum, the longitudinal muscle is innervated by excitatory (8,9,10) and inhibitory motor neurons (11). Excitatory motorneurons release primarily acetylcholine (12) and the acetylcholine-containing neurons can be selectively labeled by antibodies raised against choline acetyltransferase (ChAT) or the vesicular acetylcholine transporter (VAChT) (13,14,15,16). Nitric oxide (NO) is a neurotransmitter used by inhibitory motorneurons along with ATP, VIP and PACAP (11). These neurons contain nitric oxide synthase (NOS), which synthesizes NO (17). NO diffuses to adjacent smooth muscle cells causing relaxation via activation of cyclic guanosine monophosphate (cGMP) dependent pathways (18). In the ENS, HuC/D (Hu)- immunoreactivity (ir) is found in all neurons (19) and antibodies against Hu have been used as a pan-neuronal parker in the myenteric plexus of guinea pig ileum (20). In myenteric plexus of guinea pig ileum, calbindin-ir is only found in intrinsic primary afferent neurons (21,22). It is worth noting that postnatal neurogenesis may occur in the myenteric plexus as there are postnatal increases in total number of myenteric neurons occur at least in the rat small intestine (23,24). In addition, postnatal gut neural crest stem cells were also isolated in the same species (25) and more importantly, enteric neurogenesis was demonstrated in adult mice (26).

Intercellular signaling in the ENS has been studied using electrochemical methods (27,28,29,30,31) where release of signaling molecules can be measured in real time (32,33,34,35,36). This is an important tool since it allows direct measurements of electroactive signaling molecules in real time near release sites. Pharmacological studies in the guinea pig ileum showed that inhibitory neuromuscular transmission to longitudinal muscle was relatively more effective in neonates (1). NOS nerve fibers supplying the longitudinal muscle had higher level of NOS-ir in neonatal animals (1), however, quantification of NOS-ir nerve fibers in this region is difficult as they are very sparse (1,8,9,10). Therefore, we used electrochemical methods to quantify the amount of NO directly adjacent to longitudinal smooth muscle. We also examined NOS expression in the longitudinal muscle and myenteric plexus in order to identify the mechanism that lays behind the relative stronger inhibitory influence in neonatal gut in guinea pig ileum.

MATERIALS AND METHODS

Animals

Animal use protocols were approved by the Institutional Animal Use and Care Committee at Michigan State University. Neonatal guinea pigs (≤48 hours postnatal, 75 – 90 g) and young adult guinea pigs (3 – 4 weeks, 300 – 400 g) were obtained from Bioport, Inc. (Lansing, MI). At 300–400 g guinea pigs are sexually mature (http://netvet.wustl.edu/species/guinea/guinpig.txt).

Diamond Microelectrode Preparation

Boron-doped diamond (BDD) thin film was deposited on a sharpened 40 µm diameter Pt wire (99.99%, Aldrich Chemical, Milwaukee, WI) by plasma-assisted chemical vapor deposition (1.5 kW, 2.54 GHz, ASTeX, Woburn, MA; 27,37). The diamond-coated Pt wire

was affixed to a copper wire using conductive Ag epoxy and the assembly was insulated with polypropylene from a pipette tip. The insulation was applied by inserting the microelectrode into a pipette tip with about a 500 µm length of the diamond-coated wire protruding from the end and carefully heating the tapered end using the coil of micropipette puller. This softened the polypropylene and caused it to flow evenly over the diamond surface. The resulting microelectrode was conically shaped with diameter at the narrowest point of approximately 10 µm and at the widest point of approximately 40 µm. The length of the exposed electrode was 100 to 200 µm.

Electrochemical measurement of nitric oxide

Guinea pigs were anesthetized via halothane inhalation, stunned and exsanguinated by severing the major neck blood vessels. A segment of ileum was harvested 15 – 20 cm proximal to the ileocecal junction and placed in an oxygenated (95% O_2 and 5% CO_2) Krebs' buffer solution, pH 7.4 of the following composition (in millimolars): 117 NaCl, 4.7 KCl, 2.5 $CaCl_2$, 1.2 $MgCl_2$, 1.2 NaH_2PO_4, 25 $NaHCO_3$ and 11 glucose. Both neonatal and adult tissue were consequently dissected and mounted in a recording chamber as described previously (30). The tissue was constantly perfused with Krebs buffer in the recording chamber at a flow rate of 2 ml min^{-1}. Continuous amperometric (CA) recording of NO was made from myenteric ganglia and longitudinal muscle using a three-electrode configuration as described before (30). NO was detected as oxidation current using a 40 µm diameter BDD microelectrode. A Pt wire served as the counter electrode and a "no leak" Ag|AgCl electrode (EE009; ESA Biosciences, Inc., Chelmsford, MA, USA) was used as the reference electrode. All amperometric measurements were performed using a BioStat™ multi-mode potentiostat (ESA Biosciences, Inc). The BDD microelectrode was reproducibly positioned over the tissue using a micromanipulator (Model 25033; Fine Scientific Tools, Foster City, CA, USA).

For NO detection, the BDD electrode was held at a detection potential of 1.0 V vs a Ag|AgCl reference electrode. At this potential, NO is oxidized at a mass transport limited rate (30). Nicotine (1 µM) was applied to the tissue by means of a superfusion pipette at a flow rate of 0.2 ml min^{-1}, which was placed within 100 µm of the BDD electrode location. Tissues were continually perfused with oxygenated Krebs' buffer kept at 37 °C and in 20 s intervals the solution containing nicotine in Krebs' buffer was perfused over the tissue. The NOS antagonist, nitro-L-arginine (NLA, 100 µM), was used to inhibit NO production. The sodium channel blocker, tetrodotoxin (TTX; 0.1 µM), was used to verify the neural dependence of NO release.

Immunohistochemistry

After guinea pigs were sacrificed, segments of ileum were immediately removed from the animals and placed in phosphate-buffered saline (PBS 0.01 mol/L, pH, 7.2) containing the L-type calcium channel blocker nifedipine (1 µM) to relax the muscle. Ileal segments were cut open along the mesenteric border, stretched and pinned flat in a silcone elastomer-lined Petri dish, which was then filled with Zamboni's fixative (2% [vol/vol] formaldehyde and 0.2% [vol/vol] saturated picric acid in PBS). Tissues were fixed overnight (4 °C) and then washed 3 times with DMSO at 10-minute intervals, followed by 3 washes in PBS at 10-minute intervals. Wholemount LMMP preparations were dissected and then preincubated in 4% normal donkey serum in PBS for 30 min at room temperature. The primary antiserums used in this study are summarized in Table 1.

All primary antiserum were diluted to 1:200 in PBS. Tissue was incubated with the first antibodies for overnight at room temperature. The excess serum was washed off with 3×10 min changes in PBS. The preparations were then incubated in fluorescein conjugated

secondary antibodies (Jackson USA) reconstituted in PBS for 2 h at room temperature. The tissue was washed in PBS for 3×10 mins and then mounted in buffered glycerol (pH = 8.6) for fluorescence microscopy. Staining was viewed using a Nikon fluorescence microscope (model TE 2000-U), and images were acquired and analyzed using MetaMorph software. In some studies, tissues from adult and neonatal animals were processed under the same conditions and the descriptive comparison between the results was made by 2 independent blinded observers. Intensity of immunoreactivity was also analyzed as arbitrary gray value unit (AGVU) using Image J Software (http://rsb.info.nih.gov/ij/) in some studies.

Western Blot

Western blot analysis was performed on total protein extracted from LMMP from neonatal and adult guinea pigs. Ileal segments were placed in cold (4°C) PBS (pH = 7.2) and LMMP was teased off with a cotton swab as described previously (1,11) at 4°C. The tissue was then lysed on ice in lysis buffer (10 mM HEPES, 150 mM NaCl, 1 mM EDTA, 0.2% NP40), containing a commercially available protease inhibitor cocktail (Cat #P8340, Sigma-Aldrich Inc., St. Louis, MO). Lysates were centrifuged at $700 \times g$ for 10 minutes at 4°C to pellet nuclear proteins and any insoluble debris. The supernatant obtained from each animal was saved separately, and total protein in the supernatant was determined using a protein assay kit (Bio-Rad, Hercules, CA). Equal amounts of protein from each sample described above were mixed with Laemmli buffer (16% mercaptoethanol [wt/vol], 6% SDS [wt/vol], 0.1% bromphenol blue [wt/vol], 30% glycerol [wt/vol], 240 mmol/L Tris, pH 6.8), separated on a 10% SDS-PAGE gel and then transferred to a nitrocellulose membrane at 4°C overnight. Membranes were blocked with 4% skim milk powder in PBS-Tween 20 buffer for 3 hours and then incubated at 4°C overnight with the primary anti-NOS antibody raised in sheep serum (Cat #AB1529, Millipore, USA; 1:1500 dilutions). This antibody is derived from the neuronal form of NOS from rat cerebellum. After overnight incubation, the membrane was washed with PBS and then further incubated for 1 hour at 4°C with a horseradish peroxidase-conjugated secondary antibody. The NOS-ir was detected by a chemiluminescence kit (Pierce, Rockford, IL). All membranes were stained with Coomassie Blue to verify equal protein loading and to quantitate total protein in each lane. The intensity of NOS bands and total protein on membranes was quantitated using Image J software (http://rsb.info.nih.gov/ij/). NOS levels in each lane were normalized to the total protein in that lane.

Measurements of distances from ganglia to NO detection sites

For some electrochemical measurements, the electrode was placed in-between the ganglia to record levels of NO production. Therefore the distance between ganglia to detection sites was calculated using nNOS immunohistochemistry images taken at ×4 magnification using Image J Software (http://rsb.info.nih.gov/ij/). Distances of from ganglia to detection sites were determined for adult and neonatal tissues.

Measurement of the gut length/area

The entire small intestine was collected from euthanized guinea pigs using a cotton string to mark the proximal and distal ends of the intestine. The small intestine was quickly transferred to phosphate-buffered saline (PBS 0.01 mol/L, pH, 7.2) containing the L-type calcium channel blocker nifedipine (1 μM), making sure that the cotton string always aligned with the small intestine. At the pylorus, the small intestine was cut with the string together so that length of the cotton string was exactly the same as the length of the gut. The length of string was documented at the end of each experiment to refer the length of the gut.

After the entire small intestine was taken, an ileal segment of 5 cm was harvested 15 to 20 cm proximal end of ileum. The ileal segment was cut open, stretched and fixed as described

above. After the tissue was washed in DMSO and PBS as described above, the area of the fixed tissue was calculated by length $\times$ width. The entire gut area was eventually calculated from the area of the ileal segment of 5 cm long.

Cell/ganglia count on myenteric plexus

Firstly, number of cells was estimated in 9 mm^2 starch-and-fixed LMMP preparations. In this part of work, double staining with NOS and Hu antibodies was performed in myenteric neurons so that number of NOS-containing neurons in every 100 Hu neurons (NOS in 100 Hu) or number of NOS-containing neurons in area of 9 mm^2 (NOS in 9 mm^2) was counted. In addition, double staining of calbindin- and Hu- neurons was also performed in this part of work so that number of calbindin-containing neurons in every 100 Hu neurons (CalB in 100 Hu) or number of calbindin-containing neurons in area of 9 mm^2 (CalB in 9 mm^2) was counted. Subsequently, the number of Hu neurons within every 9 mm^2 LMMP preparation (Hu in 9 mm^2) was calculated by the following two methods:

$$(\text{NOS in 9 mm}^2) \times \frac{100}{\text{NOS in 100 Hu}} \tag{1}$$

and

$$(\text{CalB in 9 mm}^2) \times \frac{100}{\text{CalB in 100 Hu}} \tag{1}$$

where (1) and (2) are estimate from NOS neurons and calbindin neurons respectively.

Secondly, number of neurons was extrapolated in starch-and-fixed LMMP preparations made from 5 cm ileal segments (Hu in 5 cm segment) using the following relationship:

$$(\text{Hu in 9 mm}^2) \times \frac{\text{Area of fixed tissue}}{9}$$

where the Hu in 9 mm^2 used the estimate of both (1) and (2); the area of fixed tissue from a 5 cm ileal segment was derived as described above.

Finally, the number of Hu neurons in the entire small intestine without being starch-and-fixed was calculated by the formula:

$$(\text{Hu in 5 cm segment}) \times \frac{\text{Length of entire small intesine}}{5}$$

where the Hu in 5 cm segment was the estimate derived from both (1) and (2) therefore number of Hu neurons in the small intestine was extrapolated from NOS- and calbindin-neurons.

In these experiments, number of ganglia was also counted in every 9 mm^2 LMMP. In some experiments, double staining was performed between antibodies for NOS and calbindin or antibodies for Chat and NOS. In those experiments, the number of NOS neurons was directly expressed against to the number of calbindin neurons. Similarly, the number of acetylcholine neurons was expressed directly against the number of NOS neurons. In addition, the number of acetylcholine neurons was counted in 9 mm^2 LMMP preparations.

Drugs

Acetylcholine (A6625), nicotine (N5260), N_ω-nitro-L-arginine (NLA; N5501) and tetrodotoxin (TTX; T5651) were all obtained from Sigma Chemical Company (St. Louis, MO).

Data analysis

All data are expressed as mean ± standard error where "n" values refer to the number of animals from which the data were obtained. Data from different treatment groups were compared using Student's *t*-test or analysis of variance (ANOVA) where appropriate. *P* < 0.05 was considered statistically significant.

RESULTS

The length and area of the entire small intestine were calculated for both neonatal and adult guinea pigs (Table 2). The density of myenteric neurons and the density of myenteric ganglia in the small intestine were also calculated for guinea pigs of the same age groups (Table 2). In neonatal animals, the density of neurons and ganglia in the myenteric plexus was more than 2 times higher than in adult animals (Table 2). The length of small intestine also doubled from neonatal to adult animals (Table 2). The area of small intestine increased more than 3 times from neonates to adults (Table 2).

Real time measurement of NO

When microelectrodes were placed within 20 µm of a myenteric ganglion, nicotine (1 µM) induced oxidation currents were detected at a potential of 1 V vs Ag|AgCl in ileal LMMP from neonatal and adult animals. When the electrode was ≥60 µm from the ganglion, no oxidation current was detected. When the electrode potential was 750 mV, no oxidation current was detected indicating that there was no interference arising from oxidation of biogenic amines. The mean nicotine-induced oxidation currents detected in adult and neonatal tissues when the electrode was placed over ganglia were 126 ± 21 and 388 ± 28 pA (P<0.05), respectively. The nicotine (1 µM)-induced oxidation currents were blocked by TTX (0.1 µM) and NLA (100 µM; Fig. 1A), confirming that neurogenically released NO was monitored. When the microelectrode was positioned between ganglia, nicotine-induced, NLA-sensitive currents were only detected in neonatal preparations (Fig. 1B). The mean nicotine-induced oxidation current in neonates was 67 ± 9 pA and was blocked by NLA (100 µM; Fig. 1B). The nicotine-induced oxidation current detected near neonatal ganglia was significantly (P < 0.05, n = 6) higher than the current in adults (Fig. 1C). In neonatal guinea pigs, the oxidation current detected from ganglia was also significantly (P < 0.05, two-way ANOVA, n = 6) higher than the current detected when the electrode was positioned over the longitudinal muscle between ganglia (Fig. 1C, D).

Detection distance from myenteric ganglia to electrode position in LMMP preparations

As elevated levels of NO were observed in-between ganglia from LMMP preparations of neonatal tissue, we examined the detection distances in adult and neonatal tissues. A greater density of ganglia and terminals were observed in neonate preparations than adult preparations (Fig 2A, B; see also in Table 2 for quantitative data). Following qualitative analysis, the distance from myenteric ganglia to detection sites for adults (*n* = 26) was 125 ± 35 µm, which was significantly greater than in neonates (*n* = 48), where the distance from ganglia to detection sites was 55 ± 23 µm (P < 0.001, *t*-test, Fig. 2C).

NOS-ir in myenteric neurons and NOS level in LMMP preparations

We next examined NOS-ir in myenteric neurons and in LMMP preparations. NOS-ir neurons were observed in neonatal and adult LMMP preparations that were fixed, stained and image-captured under identical conditions (Fig. 3A, B). The density of NOS-ir neurons in neonatal tissues (Fig. 3A) was higher than in adult tissues (Fig. 3B). The intensity of NOS-ir in the neonatal neurons (Fig. 3A) was also higher than that in the adult neurons (Fig. 3B).

Western blot analysis was also used to compare the relative expression of NOS in the LMMP preparations made from neonatal (n = 4) and adult (n = 3) guinea pigs (Fig. 3C, D). In extracts from both neonatal and adult LMMP preparations, Western blot revealed a prominent band near 105 kD (Fig. 3C). Quantitative assessment showed that the intensity of the 105 kD band was significantly ($P < 0.05$, t-test, n = 3 to 4) greater in neonatal samples compared with samples from adults (Fig. 3D).

Nicotinic receptors

It is possible that the higher nicotine-induced NO oxidation current in neonatal tissues was due to higher nicotinic acetylcholine receptor (nAChR) expression in neonates. Therefore, we compared the expression of α3/α5 subunits of nAChRs using immunohistochemical methods and LMMP preparations made from neonatal and adult animals (Fig. 4E, F). Preparations made from adult and neonatal animals were fixed, processed, stained and camera-captured under the same conditions. Based on an average of 5 nAChR-ir positive neurons from each animal age group, quantitative analysis showed that the intensity of nAChR-ir in myenteric neurons in neonates and adults was 81.2 ± 5.2 and 82.7 ± 3.1 (AGVU) respectively (n = 3–4). The intensity of nAChR-ir in myenteric neurons was not significantly ($P > 0.05$, unpaired t-test; n = 3–4) different between neonates and adults.

Number of myenteric neurons

The total number of NOS neurons in the small intestine of neonatal guinea pigs was $860,000 \pm 20,000$ and the total number of NOS neurons in adult guinea pig was $760,000 \pm 50,000$. The total numbers of NOS neurons in neonatal and adult animals were not significantly different ($P > 0.05$, t-test, n = 5–6; Fig. 5A). The number of calbindin neurons in the entire small intestine of neonatal and adult guinea pigs was also calculated (Fig. 5B; example of calbindin-ir in neonatal preparation in Fig. 4A). The total number of calbindin neurons in neonatal guinea pig was $870,000 \pm 40,000$ and the total number of calbindin neurons in adult guinea pig was $940,000 \pm 100,000$. The total number of calbindin neurons in neonatal and adult animals was not different ($P > 0.05$, t-test, n = 5–6; Fig. 5A).

The number of myenteric neurons in the entire small intestine was estimated from NOS neurons and calbindin neurons (Fig. 5A, B). The number of myenteric neurons in adult small intestine estimated from NOS neurons or calbindin neurons was 4.6 ± 0.3 and 4.8 ± 0.3 million respectively. The number of myenteric neurons in neonatal small intestine estimated from NOS neurons or calbindin neurons was 3.4 ± 0.2 and 3.5 ± 0.3 million, respectively. The number of myenteric neurons estimated from NOS neurons and calbindin neurons was not significantly ($P > 0.05$, t-test, n = 5 to 6) different in either adult or neonatal animals (Fig. 5A, B). From both estimates, the number of myenteric neurons in the adult intestine was significantly higher than in the neonatal intestine ($P < 0.05$, unpaired t-test, n = 5 – 6; Fig. 5A, B).

The percentage of either NOS or calbindin neurons in the small intestine was estimated for both adult and neonatal guinea pig (Table 3). The percentage of NOS neurons was $17 \pm 1\%$ and $26 \pm 2\%$ in adult and neonates respectively while the percentage of calbindin neurons

was $21 \pm 3\%$ and $25 \pm 2\%$ in adult and neonates respectively. The percentage of NOS neurons was significantly higher in neonatal animals (P < 0.05, *t*-test, n = 5–6; Table 3), however, the percentage of calbindin neurons was not different (P > 0.05, *t*-test, n = 5–6) different between the adult and neonatal animals (Table 3). The density (neurons per mm^2) of NOS and calbindin neurons in the small intestine was calculated for both adult and neonatal guinea pigs (Table 3). The density of NOS neurons was 27 ± 2 neurons per mm^2 and 97 ± 8 neurons per mm^2 in adult and neonates respectively. The density of calbindin neurons was 34 ± 3 neurons per mm^2 and 101 ± 7 neurons per mm^2 in adult and neonates respectively (Table 3). NOS and calbindin neuronal density was lower in adults (P < 0.05, *t*-test, n = 5–6).

NOS-ir neuron number was expressed as a percentage of the number of calbindin neurons counted in preparations immunohistochemically double-labeled for both markers (Fig. 5C). This percentage was 157 ± 7 % in neonates and $122 \pm 5\%$ in adults. In this assay, the ratio between the number of NOS and calbindin neurons was significantly (P < 0.05, *t*-test, n = 6) lower in adult animals (Fig. 5C). Number of cholinergic neuron was also expressed as a percentage of the number of calbindin neurons counted in preparations immunohistochemically double-labeled for both markers (Fig. 5D; example of ChAT-ir in neonatal preparation in Fig. 4B). This percentage was $175 \pm 30\%$ in neonates and $99 \pm 22\%$ in adults; this difference was not statistically significant (P > 0.05, unpaired *t*-test, n = 5; Fig. 5D).

Cholinergic nerve fibers were examined in neonatal and adult tissues using a VChAT antibody (Fig. 4C, D). Single staining of VAChT revealed that cholinergic nerve fibers were abundant in myenteric ganglia and in the tertiary plexus in neonatal and adult tissues (Fig. 4C, D). The density of cholinergic nerve fibers was higher in neonatal tissue (Fig. 4C) compared to adult tissues (Fig. 4D). The intensity of VAChT-ir in the neonatal cholinergic fibers (Fig. 4C) was also higher than that in the adult cholinergic fibers (Fig. 4D).

DISCUSSION

In this study, we directly measured the level of NO, in real time, from both neonatal and adult LMMP preparations using continuous amperometry. Continuous amperometry has been used to monitor neurotransmitter release *in vivo* and *in vitro* (32,33,34,35,36). This method measures transient changes in electroactive neurotransmitters near release sites. Using this method, NO oxidation currents have been recorded from a variety of tissues (39,40,41) including myenteric ganglia in guinea pig ileum (30).

One important finding of this study is that the neuronal NO production in response to nicotine stimulation was greater in neonatal compared to adult LMMP preparations. The greater response does not appear to be due to age-related differences in nAChR expression but many other factors could contribute to this functional difference. However, it is known the electrical field stimulation evoked NANC relaxations of the longitudinal muscle are larger in neonatal (1). In addition, we show that NOS-ir is more prominent in neurons and nerve fibers in neonatal tissues and that quantitative assessment by Western blot reveals higher NOS levels in neonatal tissues. Therefore, the contribution to elevated levels of NO oxidation currents in the neonate compared to the adult is due at least in part to higher NOS expression in the neonatal intestine.

Our electrochemical results also revealed that detection of NO over the myenteric ganglia and longitudinal muscle is more uniform in neonatal tissue with respect to adult tissue. NO oxidation currents were detected when the electrode was positioned over myenteric ganglia or over the tertiary plexus in neonatal tissues. NO oxidation currents were detected only

when the electrode was positioned over myenteric ganglia in adult tissues. This correlates with a higher density of NOS-ir nerve fibers in the tertiary plexus in neonates compared to adult tissues. However, we estimated that NO oxidation currents arising from NO release in myenteric ganglia can be detected at distances up to 60 µm from the source (42). Therefore, it is possible that the increased NO current detected in the tertiary plexus in neonates is due partly to a contribution of NO diffusing from myenteric ganglia as the interganglionic distance was much smaller in neonatal (54 µm) compared to adult (127 µm) tissues. This result is consistent with our overall conclusion that the muscle layers in the neonatal gut are under stronger inhibitory control compared to adult animals (1).

Although the intensity of NOS-ir in myenteric neurons was not quantified in this study, quantitative assessment by Western blot showed that level of NOS expression in the entire LMMP preparations was significantly higher in neonates. Given that there are few NOS fibers in regions outside ganglia in LMMP preparations (1,8,9,10), the quantitative assay by Western blot should largely reflect the NOS level in NOS neurons. It is worth noting that the Western blot in this study revealed a prominent band at around 105 kD instead of 160 kD, which is the predicted molecular weight of neuronal NOS in guinea pig (43). It is possible that the protease inhibitor used in protein isolation was not sufficient to fully block the protease activity and the 105-kD band represented a degradation product of the NOS protein. The antibody used in the Western blot study was derived from a sequence of neuronal NOS of rat cerebellum. A similar NOS antibody was used in a previous study in which the antibody predominantly recognized lower molecular weight proteins compared to other nNOS antibodies tested (44).

Another important finding of this study was that postnatal neurogenesis could play a crucial role in the maturation of ENS. The age-related decline in the relative strength of the inhibitory innervation of the muscle layers could be due to loss of NOS-ir neurons. This is not likely to be the case since little apoptosis has been detected in myenteric neurons in the guinea pig intestine (45). An alternative possibility is that inhibitory neurons are diluted postnatally by other neurons generated after birth. Postnatal neurogenesis has been suggested in both central nervous system (46,47,48,49) and peripheral nervous system (50,51) including enteric nervous system (23,24,25,26). In this study, number of myenteric neurons was compared between adult and neonatal animals. Total number of myenteric neurons has been previously evaluated in guinea pig ileum (see examples in 52,53). In this study, Hu antibody was used as a marker for all myenteric neurons (20). Hu positive cells are all clustered together in myenteric ganglia, making accurate cell counts difficult. Therefore, subtypes of enteric neurons were counted and these counts were used to extrapolate the number of Hu-containing neurons. In this study, number of myenteric neurons was extrapolated from NOS- and calbindin-containing neurons based on estimates obtained from 5 cm lengths of ileum taken 15 cm proximal to the ileocecal junction. It is possible that this method yield some inaccuracies as the density of NOS neurons in the guinea pig duodenum is reported to be lower than in the ileum (54). However, this study is not aimed at a precise number of the total myenteric neurons within the system but a consistent sampling procedure for statistics to determine the likelihood that there is a relative increase in the number of myenteric neurons as the animals mature postnatally. In estimates made from either NOS- or calbindin-neurons, the number of myenteric neurons in adult was significantly higher than it was in neonates indicating a postnatal neurogenesis in the myenteric plexus.

Due to postnatal neurogenesis, the percentage of NOS neurons declined significantly from neonatal to adult animals without a change in the total number of NOS neurons. This suggests that NOS neurons were diluted by newly-generated myenteric neurons. Calbindin neurons did not increase significantly during postnatal neurogenesis when the cell counts

were compared between neonate and adult tissues. However, when the percentage of neurons was examined in light of postnatal neurogenesis, the proportion of calbindin neurons did not change. Therefore, the number of calbindin neurons was not as constant as NOS neurons and some calbindin neurons may have arisen from postnatal neurogenesis. It is also possible that there are small changes in the level of expression of calbindin between neonates and adults allowing more calbindin neurons to be detected. This change in expression could confound calculations of the number of calbindin neurons.

In the guinea pig ileum, calbindin and NOS mark sensory and inhibitory motorneurons respectively (21,22,55). To eliminate the sensory-neuron-induced variability, the number of NOS neurons was expressed against number of calbindin neurons (NOS/CalB) so that the ratio of NOS/CalB can be a measure for changes in inhibitory neurons. The NOS/CalB ratio was higher in neonates compared to adults, suggesting a decline in NOS neurons in the maturing guinea pig ileum, regardless of any postnatal changes in calbindin neurons.

The number of acetylcholine containing neurons (ChAT-ir) was expressed against calbindin neurons. In the myenteric plexus, acetylcholine is contained in almost all neuronal subtypes except inhibitory motorneurons (55). Hence, the ratio of Chat/CalB is a measure of non-inhibitory neurons. Although the ratio of Chat/CalB declined during postnatal development, the decline was not statistically significant. This suggests that the non-sensory cholinergic component did not decline due to postnatal neurogenesis. We did not calculate the percentage of ChAT neurons. However as the percentages of NOS neurons in adult and neonates are 17% and 26% respectively, ChAT neurons as a percentage all myenteric neurons should be about 83% in adult and 74% in neonates assuming that all neurons contain either NOS or ChAT. Direct assessment of the number of ChAT neurons is needed to determine if there are postnatal changes in the number of these important neurons.

A postnatal increase in cholinergic neurons has been suggested by a previous study in which few cholinergic nerve fibers were detected in the circular muscle of the neonatal mouse colon (2). In the guinea pig ileum however, both the density of acetylcholine fibers and intensity of VAChT-ir in cholinergic fibers were higher in neonatal tissue. This is consistent with our previous pharmacological data in which the nicotine-induced muscle contraction is higher in neonates (1). It is possible that excitatory neurotransmission to longitudinal muscle cells was also stronger at the neonatal stage since the density of both ganglia and neurons in myenteric plexus are higher in neonates. The length and area of ileum underwent tremendous growth during postnatal development, which should contribute not only to reduced density of myenteric neurons but also reduced intensity of neuronal markers. Taken together our data indicate that both excitatory and inhibitory neuronal input to longitudinal muscle cells is greater than neonatal intestine. However, the inhibitory innervation of the longitudinal muscle is relatively more effective in neonatal guinea pig ileum. During the postnatal maturation, inhibitory neurons are diluted by other type of neurons that arrive after birth.

SUMMARY AND CONCLUSIONS

In summary, more NO is released from inhibitory neurons to longitudinal muscle cells in the neonatal guinea pig ileum than the adult guinea pig ileum. Inhibitory motor neurons are postnatally diluted by postnatal neurogenesis of yet unidentified neuronal subtypes. Delayed maturation of the ENS may contribute to pediatric motility disturbances.

Acknowledgments

has been previously published in abstract form in AMS 2006 (Neurogastroenterol Motil. 2006 Aug; 18(8): 663–798).

References

1. Bian X, Burda JE, Carrasquillo M, Galligan JJ. Postnatal downregulation of inhibitory neuromuscular transmission to the longitudinal muscle of the guinea pig ileum. Neurogastroenterol Motil. 2009; 21:969–977. [PubMed: 19374637]

2. Roberts RR, Murphy JF, Young HM, Bornstein JC. Development of colonic motility in the neonatal mouse-studies using spatiotemporal maps. Am J Physiol Gastrointest Liver Physiol. 2007 Mar; 292(3):G930–G938. [PubMed: 17158255]

3. DeVries P, Soret R, Sarnacki S, Roze J, Heloury Y, Neunlist M. Postnatal changes in the neurochemical phenotype and impact on colonic motor response in the newborn rat. Neurogastroenterol Motil. 2008; 20 Supplement 1:19. [PubMed: 18031473]

4. Arce DA, Ermocilla CA, Costa H. Evaluation of constipation. Am Fam Physician. 2002 Jan 1; 65(11):2283–2290. [PubMed: 12074527]

5. Felt B, Wise CG, Olson A, Kochhar P, Marcus S, Coran A. Guideline for the management of pediatric idiopathic constipation and soiling. Multidisciplinary team from the University of Michigan Medical Center in Ann Arbor. Arch Pediatr Adolesc Med. 1999 Apr; 153(4):380–385. [PubMed: 10201721]

6. Berseth CL. Gastrointestinal motility in the neonate. Clin Perinatol. 1996 Jun; 23(2):179–190. [PubMed: 8780900]

7. Furness, JB. The Enteric Nervous System. 1st Edn. Oxford, UK: Blackwell Publishing; 2006.

8. Brookes SJ, Song ZM, Steele PA, Costa M. Identification of motor neurons to the longitudinal muscle of the guinea pig ileum. Gastroenterology. 1992 Sep; 103(3):961–973. [PubMed: 1379956]

9. Costa M, Brookes SJ, Steele PA, Gibbins I, Burcher E, Kandiah CJ. Neurochemical classification of myenteric neurons in the guinea-pig ileum. Neuroscience. 1996 Dec; 75(3):949–967. [PubMed: 8951887]

10. Pompolo S, Furness JB. Sources of inputs to longitudinal muscle motor neurons and ascending interneurons in the guinea-pig small intestine. Cell Tissue Res. 1995 Jun; 280(3):549–560. [PubMed: 7606768]

11. Osthaus LE, Galligan JJ. Antagonists of nitric oxide synthesis inhibit nerve-mediated relaxations of longitudinal muscle in guinea pig ileum. J Pharmacol Exp Ther. 1992 Jan; 260(1):140–145. [PubMed: 1370537]

12. Cousins HM, Edwards FR, Hirst GD, Wendt IR. Cholinergic neuromuscular transmission in the longitudinal muscle of the guinea-pig ileum. J Physiol. 1993 Nov.471:61–86. [PubMed: 8120825]

13. Schemann M, Sann H, Schaaf C, Mäder M. Identification of cholinergic neurons in enteric nervous system by antibodies against choline acetyltransferase. Am J Physiol. 1993 Nov; 265(5 Pt 1):G1005–G1009. [PubMed: 8238509]

14. Steele PA, Brookes SJ, Costa M. Immunohistochemical identification of cholinergic neurons in the myenteric plexus of guinea-pig small intestine. Neuroscience. 1991; 45(1):227–239. [PubMed: 1721693]

15. Lomax AE, Furness JB. Neurochemical classification of enteric neurons in the guinea-pig distal colon. Cell Tissue Res. 2000 Oct; 302(1):59–72. [PubMed: 11079716]

16. Sang Q, Young HM. The identification and chemical coding of cholinergic neurons in the small and large intestine of the mouse. Anat Rec. 1998 Jun; 251(2):185–199. [PubMed: 9624448]

17. Sanders KM, Ward SM. Nitric oxide as a mediator of nonadrenergic noncholinergic neurotransmission. Am J Physiol. 1992 Mar; 262(3 Pt 1):G379–G392. [PubMed: 1347974]

18. Tepavcević SN, Isenović ER, Varagić VM, Milovanović SR. Sodium nitroprusside regulates the relaxation of the longitudinal muscle in the gut. Pharmazie. 2008 Feb; 63(2):151–155. [PubMed: 18380403]

19. Phillips RJ, Hargrave SL, Rhodes BS, Zopf DA, Powley TL. Quantification of neurons in the myenteric plexus: an evaluation of putative pan-neuronal markers. J Neurosci Methods. 2004 Feb 15; 133(1–2):99–107. [PubMed: 14757350]

20. Lin Z, Gao N, Hu HZ, Liu S, Gao C, Kim G, Ren J, Xia Y, Peck OC, Wood JD. Immunoreactivity of Hu proteins facilitates identification of myenteric neurones in guinea-pig small intestine. Neurogastroenterol Motil. 2002 Apr; 14(2):197–204. [PubMed: 11975720]

21. Furness JB, Trussell DC, Pompolo S, Bornstein JC, Smith TK. Calbindin neurons of the guinea-pig small intestine: quantitative analysis of their numbers and projections. Cell Tissue Res. 1990 May; 260(2):261–272. [PubMed: 2357722]

22. Furness JB, Jones C, Nurgali K, Clerc N. Intrinsic primary afferent neurons and nerve circuits within the intestine. Prog Neurobiol. 2004 Feb; 72(2):143–164. Review. [PubMed: 15063530]

23. Gabella G. Neurone number in the myenteric plexus in new-born and adult rats. Experientia. 1967 Jan 15; 23(1):2–3.

24. Gabella G. Neuron size and number in the myenteric plexus of the newborn and adult rat. J Anat. 1971 May; 109(Pt 1):81–95. [PubMed: 5556678]

25. Kruger GM, Mosher JT, Bixby S, Joseph N, Iwashita T, Morrison SJ. Neural crest stem cells persist in the adult gut but undergo changes in self-renewal, neuronal subtype potential, and factor responsiveness. Neuron. 2002 Aug 15; 35(4):657–669. [PubMed: 12194866]

26. Liu MT, Kuan YH, Wang J, Hen R, Gershon MD. 5-HT4 receptor-mediated neuroprotection and neurogenesis in the enteric nervous system of adult mice. J Neurosci. 2009 Aug 5; 29(31):9683–9699. [PubMed: 19657021]

27. Bertrand PP. Real-time measurement of serotonin release and motility in guinea pig ileum. J Physiol. 2006 Dec 1; 577(Pt 2):689–704. [PubMed: 16959854]

28. Patel BA, Bian X, Quaiserová-Mocko V, Galligan JJ, Swain GM. In vitro continuous amperometric monitoring of 5-hydroxytryptamine release from enterochromaffin cells of the guinea pig ileum. Analyst. 2007 Jan; 132(1):41–47. [PubMed: 17180178]

29. Bian X, Patel B, Dai X, Galligan JJ, Swain G. High mucosal serotonin availability in neonatal guinea pig ileum is associated with low serotonin transporter expression. Gastroenterology. 2007 Jun; 132(7):2438–2447. [PubMed: 17570217]

30. Patel BA, Galligan JJ, Swain GM, Bian X. Electrochemical monitoring of nitric oxide released by myenteric neurons of the guinea pig ileum. Neurogastroenterol Motil. 2008 Nov; 20(11):1243–1250. [PubMed: 18694441]

31. Keating DJ, Spencer NJ. Release of 5-hydroxytryptamine from the mucosa is not required for the generation or propagation of colonic migrating motor complexes. Gastroenterology. 2009 Sep 23. [Epub ahead of print].

32. Stamford JA. In vivo voltammetry: some methodological considerations. J Neurosci Methods. 1986 Jul; 17(1):1–29. Review. [PubMed: 3528683]

33. Kawagoe KT, Zimmerman JB, Wightman RM. Principles of voltammetry and microelectrode surface states. J Neurosci Methods. 1993 Jul; 48(3):225–240. Review. [PubMed: 8412305]

34. Travis ER, Wightman RM. Spatio-temporal resolution of exocytosis from individual cells. Annu Rev Biophys Biomol Struct. 1998; 27:77–103. Review. [PubMed: 9646863]

35. Troyer KP, Heien ML, Venton BJ, Wightman RM. Neurochemistry and electroanalytical probes. Curr Opin Chem Biol. 2002 Oct; 6(5):696–703. Review. [PubMed: 12413556]

36. Park J, Quaiserová-Mocko V, Patel BA, Novotný M, Liu A, Bian X, Galligan JJ, Swain GM. Diamond microelectrodes for in vitro electroanalytical measurements: current status and remaining challenges. Analyst. 2008 Jan; 133(1):17–24. [PubMed: 18087609]

37. Park J, Galligan JJ, Fink GD, Swain GM. In vitro continuous amperometry with a diamond microelectrode coupled with video microscopy for simultaneously monitoring endogenous norepinephrine and its effect on contractile response of a rat mesenteric artery. Anal Chem. 2006; 78:6756–6764. [PubMed: 17007494]

38. Schemann M, Sann H, Schaaf C, Mäder M. Identification of cholinergic neurons in enteric nervous system by antibodies against choline acetyltransferase. Am J Physiol. 1993 Nov; 265(5 Pt 1):G1005–G1009. [PubMed: 8238509]

39. Patel BA, Arundell M, Parker KH, Yeoman MS, O'Hare D. Detection of Nitric Oxide Release from Single Neurons in the Pond Snail, *Lymnaea stagnalis*. Anal. Chem. 2006; 78(22):7643–7648. [PubMed: 17105154]

40. Ferreira NR, Ledo A, Frade JG, Gerhardt GA, Laranjinha J, Barbosa RM. Electrochemical measurement of endogenously produced nitric oxide in brain slices using Nafion/o-phenylenediamine modified carbon fiber microelectrodes. Analytica Chimica Acta. 2005; 535(1–2):1–7.

41. Amatore C, Arbault S, Bouret Y, Cauli B, Guille M, Rancillac A, Rossier J. Nitric Oxide Release during Evoked Neuronal Activity in Cerebellum Slices: Detection with Platinized Carbon-Fiber Microelectrodes. ChemPhysChem. 2006; 7(1):181–187. [PubMed: 16353265]

42. Smith T, Philippides A. Nitric Oxide Signalling in Real and Artificial Neural Networks. BT Technology Journal. 2000; 18(4):140–149.

43. Olsson C, Chen BN, Jones S, Chataway TK, Costa M, Brookes SJ. Comparison of extrinsic efferent innervation of guinea pig distal colon and rectum. J Comp Neurol. 2006 Jun 20; 496(6): 787–801. [PubMed: 16628614]

44. Coers W, Timens W, Kempinga C, Klok PA, Moshage H. Specificity of antibodies to nitric oxide synthase isoforms in human, guinea pig, rat, and mouse tissues. J Histochem Cytochem. 1998 Dec; 46(12):1385–1392. [PubMed: 9815280]

45. Parr EJ, Sharkey KA. Multiple mechanisms contribute to myenteric plexus ablation induced by benzalkonium chloride in the guinea-pig ileum. Cell Tissue Res. 1997 Aug; 289(2):253–264. [PubMed: 9211828]

46. Alvarez-Buylla A, Garcia-Verdugo JM, Tramontin AD. A unified hypothesis on the lineage of neural stem cells. Nature Reviews. Neuroscience. 2001; 2(4):287–293.

47. Gage FH. Mammalian neural stem cells. Science. 2000; 287(5457):1433–1438. [PubMed: 10688783]

48. Goldman SA, Luskin MB. Strategies utilized by migrating neurons of the postnatal vertebrate forebrain. Trends in Neuroscience. 1998; 21(3):107–114.

49. Zhu XJ, Hua Y, Jiang J, Zhou QG, Luo CX, Han X, et al. Neuronal nitric oxide synthase-derived nitric oxide inhibits neurogenesis in the adult dentate gyrus by downregulating cyclic AMP response element binding protein phosphorylation. Neuroscience. 2006; 141(2):827–836. [PubMed: 16735094]

50. Arora DK, Cosgrave AS, Howard MR, Bubb V, Quinn JP, Thippeswamy T. Evidence of postnatal neurogenesis in dorsal root ganglion: role of nitric oxide and neuronal restrictive silencer transcription factor. J Mol Neurosci. 2007; 32(2):97–107. [PubMed: 17873293]

51. Yan H, Keast JR. Neurturin regulates postnatal differentiation of parasympathetic pelvic ganglion neurons, initial axonal projections, and maintenance of terminal fields in male urogenital organs. J Comp Neurol. 2008 Mar 10; 507(2):1169–1183. [PubMed: 18175352]

52. Young HM, Furness JB, Sewell P, Burcher EF, Kandiah CJ. Total numbers of neurons in myenteric ganglia of the guinea-pig small intestine. Cell Tissue Res. 1993 Apr; 272(1):197–200. [PubMed: 8481953]

53. Gabella G. The number of neurons in the small intestine of mice, guinea-pigs and sheep. Neuroscience. 1987 Aug; 22(2):737–752. [PubMed: 2444903]

54. Furness JB, Li ZS, Young HM, Förstermann U. Nitric oxide synthase in the enteric nervous system of the guinea-pig: a quantitative description. Cell Tissue Res. 1994 Jul; 277(1):139–149. [PubMed: 7519970]

55. Brookes SJ. Classes of enteric nerve cells in the guinea-pig small intestine. Anat Rec. 2001 Jan 1; 262(1):58–70. Review. [PubMed: 11146429]
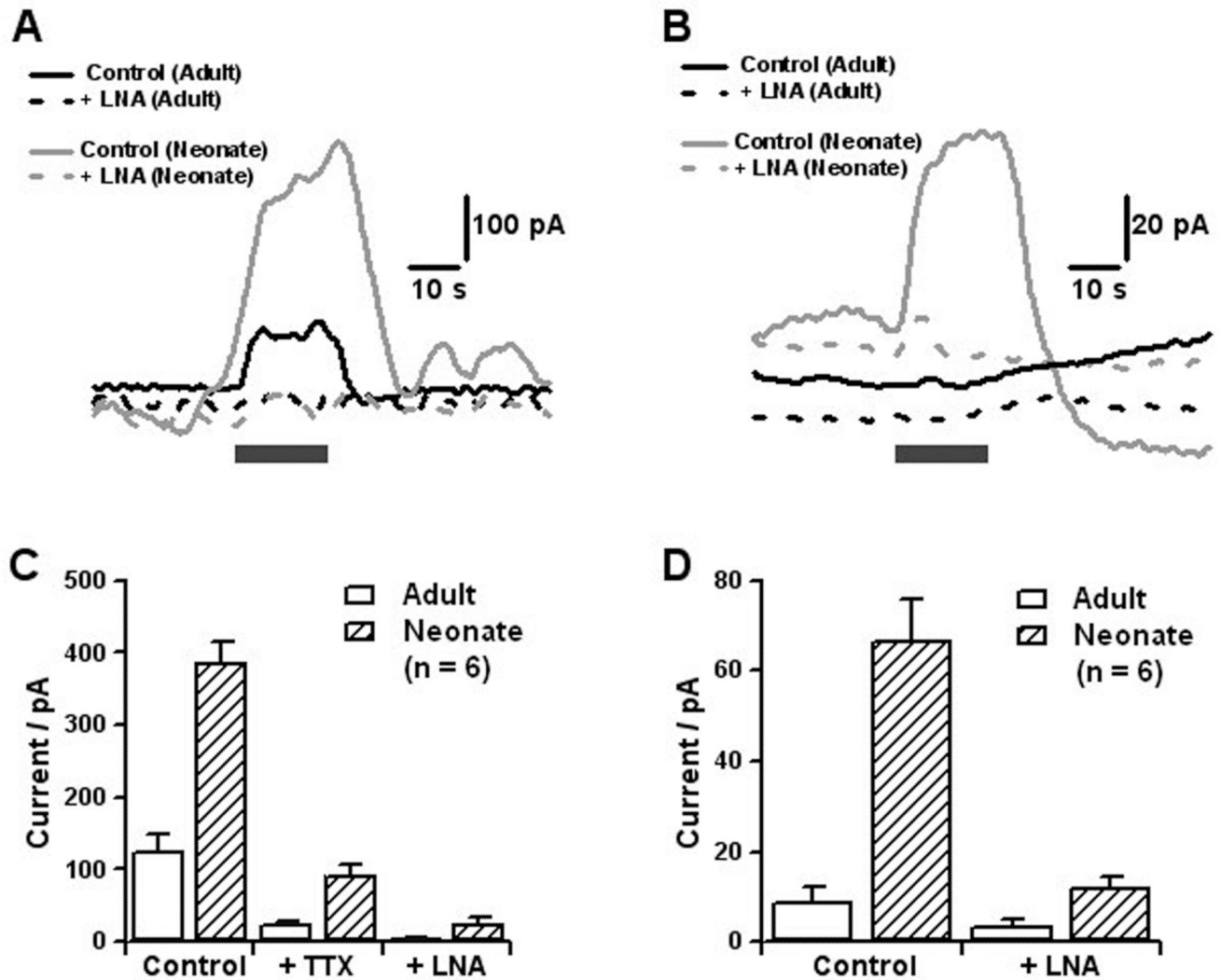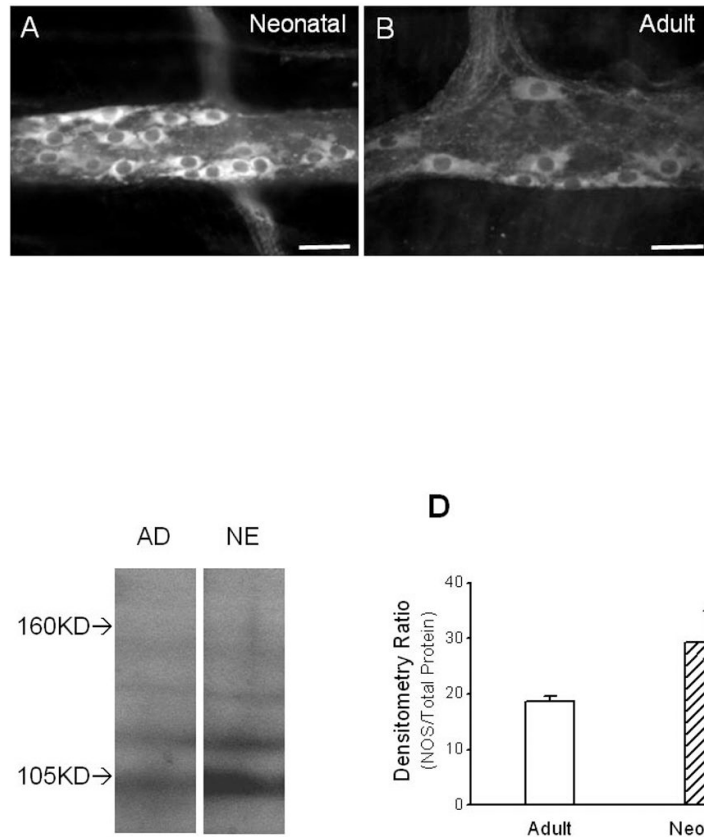
Figure 1.
Real time detection of NO in ileal LMMP made from neonatal and adult guinea pigs. [A]
and [B]: Original tracings of real time detection of NO in neonatal and adult tissues. BDD
microelectrode was positioned either over the surface of myenteric ganglia [A] or located in
between the myenteric ganglia [B]. Release of NO was induced by nicotine (1 µM). [C]:
Pooled data of real time detection of NO in control (n = 4), in the presence of TTX (100 nM)
or in the presence of NLA (100 µM). Signals detected by microelectrodes positioning over
the surface of myenteric ganglia in neonatal and adult tissues. [D]: Pooled data of real time
detection of NO in control or in the presence of NLA (100 µM). Signals detected by the
microelectrode positioning over the surface of tissue area in between ganglia in neonatal and
adult tissues. In [C] and [D], data was expressed as mean ± SEM.
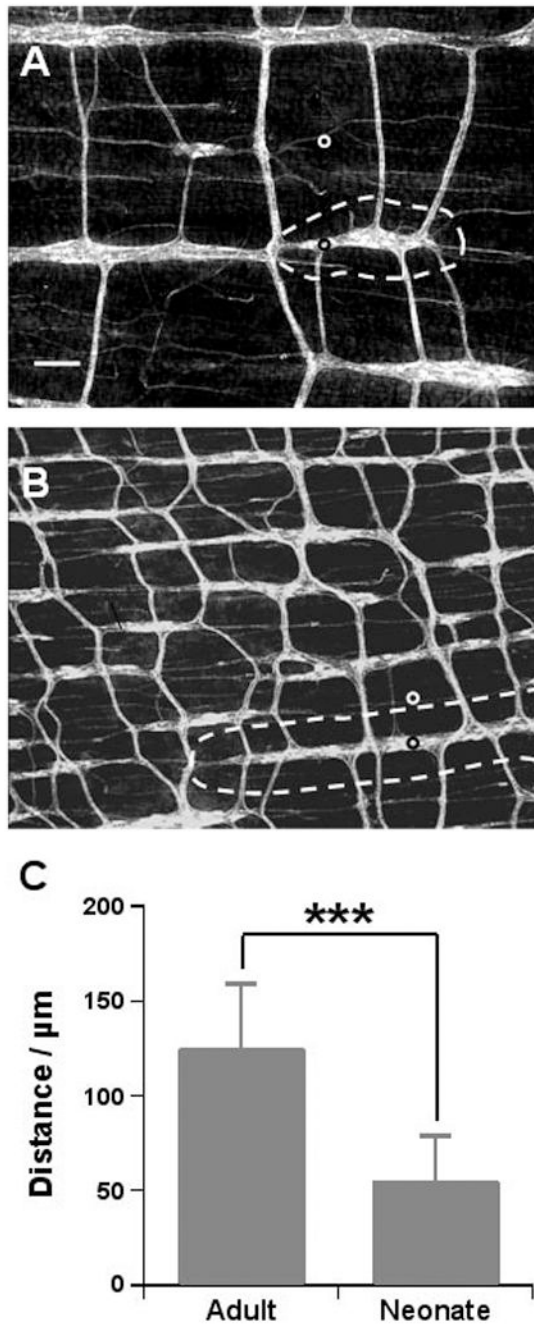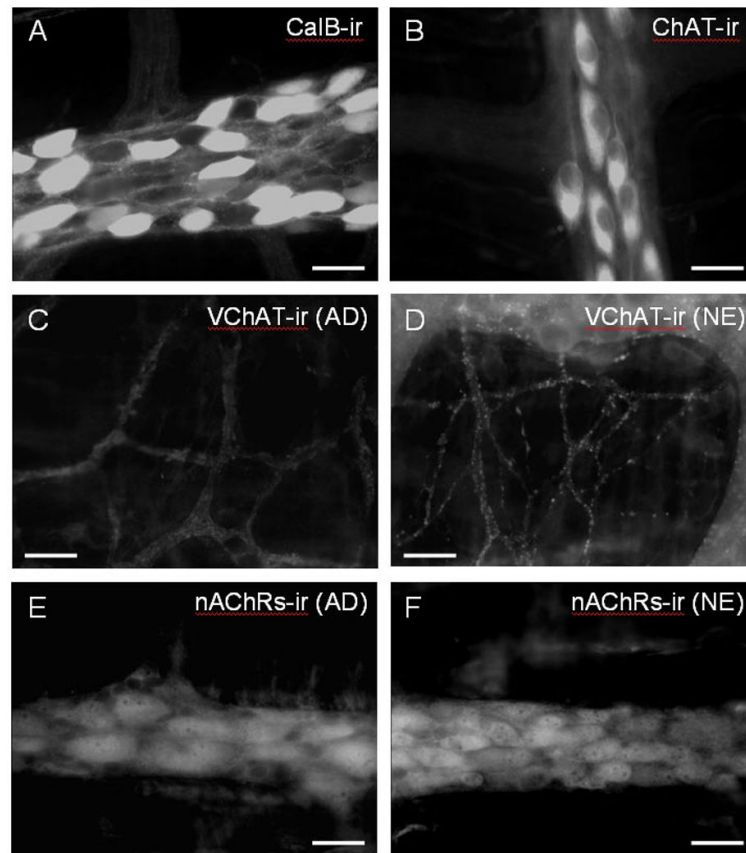
Figure 2.
Analysis of distance from myenteric ganglia to detection sites in neonatal and adult guinea pigs. [A] and [B]: Photomicrographs of NOS-ir neurons in neonatal and adult tissues. A greater density of neurons and fibers within the same tissue area was observed in neonates [B] compared to adults [A]. The black circle indicates location of ganglia measurements using the BBD electrode, whilst the white circle indicates the location the BBD sensor is placed to conduct in-between recordings of NO production. The dashed white line indicates the maximal distance of NO is observed following release based upon diffusivity and consumption from a mathematical model. Scale bar for both photomicrographs: 100 µm. [C]

The distance from myenteric ganglia to detection sites is greater in adults (n = 26) in comparison to neonates (n = 48, P < 0.001). Data expressed as mean ± SEM.

Figure 3.
Photomicrographs of NOS-ir and Western blot analysis of NOS expression in LMMP made from guinea pig ileum. Intensity of NOS-ir in myenteric neurons in neonatal tissue [A] was higher than it was in adult tissue [B]. Tissues were fixed, processed, stained and camera-captured under the same conditions. Scale bars: 20 µm. [C]: Western blot revealed a band at 105 kilodaltons that was recognized by the NOS antibody in a protein extract from both neonatal (NE) and adult (AD) guinea pigs. [D]: Densitometry performed in samples from 4 neonatal tissues and 3 adult tissues in which intensity of the 105 kilodalton band was normalized to the total protein present in each lane. Data were expressed as mean ± se. The intensity of the 105 kilodalton band was significantly greater in neonatal compared to adult tissues (P < 0.05).

Figure 4.
Photomicrographs of immunoreactivity in the myenteric plexus of guinea pig ileum. [A]: Example images of calbindin immunoreactivity in the myenteric plexus of neonatal ileum. [B]: Example images of Chat immunoreactivity in the myenteric plexus of neonatal ileum. [C] and [D]: VAChT-ir in ileal LMMP made from neonatal and adult guinea pig. Based on descriptive comparison by blinded observers, density of VAChT-ir in myenteric neurons in neonatal tissue [C] was higher than it was in adult tissue [D]. [E] and [F]: nAChRs-ir in ileal LMMP made from neonatal and adult guinea pig. Based on descriptive comparison by blinded observers, density of nAChRs -ir in myenteric neurons in neonatal tissue [E] was not different from it was in adult tissue [F]. In [C], [D], [E] and [F], tissues were fixed, processed, stained and camera-captured under the same conditions. Scale bars: 15 µm.
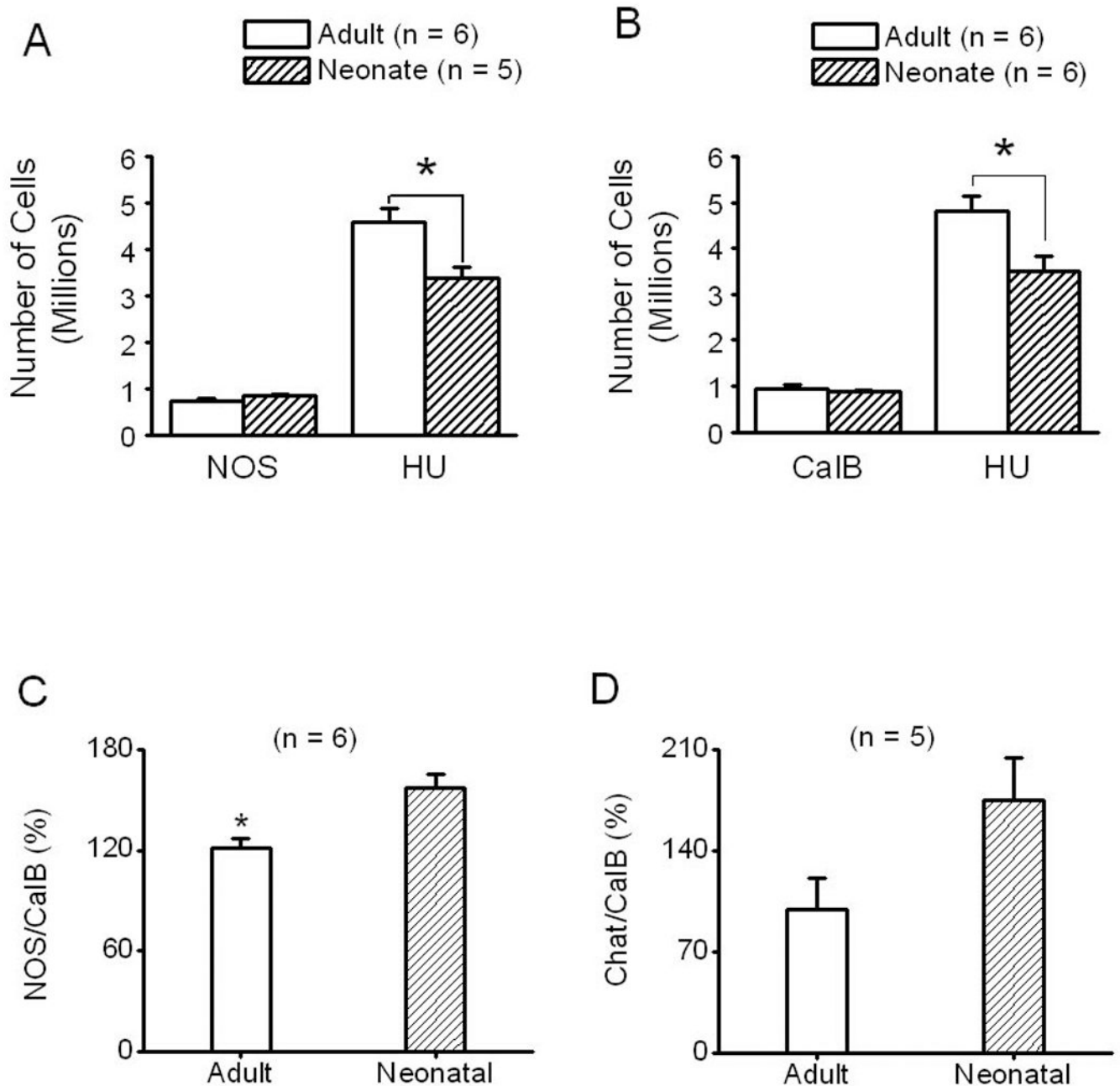
Figure 5.
Quantification of myenteric neurons in LMMP preparations made from neonatal and adult guinea pig in the small intestine. Number of total myenteric neurons was extrapolated from number of NOS positive neurons [A] and number of calbindin positive neurons [B]. In both extrapolations, the total number of myenteric neurons in adult was higher than it was in neonatal. In either neonate or adult, the total numbers of myenteric neurons extrapolated from both markers did not differ statistically. The ratio between the numbers of NOS- and calbindin-neurons (NOS/CalB) was statistically higher in neonates than it was in adult [C], however, the ratio between the numbers of acetylcholine- and calbindin- neurons (Chat/CalB) was not scientifically different between the two age groups [D].

Table 1

The primary antiserums used in this study:

Antigen	Host species	Source
Calbindin-D28K	Rabbit	Oncogene, USA (Cat. NO: PC253L)
Calbindin-D28K	Mouse monoclonal	Sigma, USA (Clone # CL-300)
NOS	Sheep	Millipore, USA (Cat. NO: AB1529)
mAB35 ($\alpha3/\alpha5$ subunits of nAChRs)	Rat	Santa Cruz Biotechnology, Inc., Santa Cruz, CA
Hu	Mouse	Molecular Probes, USA (Cat. NO: A-21271)
Chat	Rabbit	Gift from Dr. Michael Schemann (P3YEB; 38), Germany
VAChT	Goat	Phoenix Pharmaceuticals, UAS (Cat. NO: H-V007)

Table 2

The length of small intestine, the area of small intestine, the density of myenteric neurons in small intestine and the density of myenteric ganglia in small intestine in neonatal and adult guinea pigs. Each value is the mean ± se of 5 to 9 experiments.

	Length (mm)	Area (mm^2)	Ganglia/mm^2	Neurons/mm^2
Adult tissues	1554.0 ± 49.1[*]	27450.7 ± 1081.5[*]	2.1 ± 0.4	171.7 ± 8.6
Neonatal tissues	811.3 ± 25.8	8701.7 ± 611.3	5.3 ± 0.4[*]	396.5 ± 12.0[*]

Asterisks indicate significant increase (P < 0.05, unpaired *t*-test; n = 5 to 6).

Table 3

Percentage and density of NOS/calbindin neurons. Each value is the mean ± se of 5 to 6 experiments.

	% of NOS neurons	% of calbindin neurons	# of NOS neurons/mm^2	# of calbindin neurons/mm^2
Adult tissues	17 ± 1	21 ± 3	27.0 ± 1.7	34.2 ± 2.8
Neonatal tissues	26 ± 2[*]	25 ± 2	96.8 ± 8.4[*]	101.2 ± 6.7[*]

Asterisks indicate significant increase (P < 0.05, unpaired *t*-test; n = 5 to 6).